

The synthetic retinoid ST1926 as a novel therapeutic agent in rhabdomyosarcoma

Hussein Basma¹, Sandra E. Ghayad², Ghina Rammal², Angelo Mancinelli³, Mohammad Harajly¹, Farah Ghamloush¹, Loai Dweik¹, Rabab El-Eit⁴, Hassan Zalzal¹, Wissam Rabeh¹, Claudio Pisano³, Nadine Darwiche⁵ and Raya Saab^{1,4*}

¹ Children's Cancer Institute, American University of Beirut, Beirut, Lebanon

² Department of Biology, Faculty of Science, EDST, Lebanese University, Beirut, Lebanon

³ Medicinal Investigational Research, Biogem Research Institute, Ariano Irpino, Italy

⁴ Department of Anatomy, Cell Biology and Physiology, American University of Beirut, Beirut, Lebanon

⁵ Department of Biochemistry and Molecular Genetics, American University of Beirut, Beirut, Lebanon

Rhabdomyosarcoma (RMS) is the most frequent soft tissue sarcoma in children. Despite multiple attempts at intensifying chemotherapeutic approaches to treatment, only moderate improvements in survival have been made for patients with advanced disease. Retinoic acid is a differentiation agent that has shown some antitumor efficacy in RMS cells *in vitro*; however, the effects are of low magnitude. E-3-(4'-hydroxyl-3'-adamantylbiphenyl-4-yl) acrylic acid (ST1926) is a novel orally available synthetic atypical retinoid, shown to have more potent activity than retinoic acid in several types of cancer cells. We used *in vitro* and *in vivo* models of RMS to explore the efficacy of ST1926 as a possible therapeutic agent in this sarcoma. We found that ST1926 reduced RMS cell viability in all tested alveolar (ARMS) and embryonal (ERMS) RMS cell lines, at readily achievable micromolar concentrations in mice. ST1926 induced an early DNA damage response (DDR), which led to increase in apoptosis, in addition to S-phase cell cycle arrest and a reduction in protein levels of the cell cycle kinase CDK1. Effects were irrespective of TP53 mutational status. Interestingly, in ARMS cells, ST1926 treatment decreased PAX3-FOXO1 fusion oncoprotein levels, and this suppression occurred at a post-transcriptional level. *In vivo*, ST1926 was effective in inhibiting growth of ARMS and ERMS xenografts, and induced a prominent DDR. We conclude that ST1926 has preclinical efficacy against RMS, and should be further developed in this disease in clinical trials.

Rhabdomyosarcoma (RMS) is the most frequent soft tissue sarcoma, and the third most common solid tumor in children.¹ It accounts for 6% of all childhood cancers and

Key words: rhabdomyosarcoma, retinoids, ST1926, cell cycle, DNA damage, PAX3-FOXO1

Abbreviations: ARMS: alveolar RMS; AUC: area under the curve; BrdU: bromodeoxyuridine; BZ: bortezomib; C_{max} : maximum concentration; CHX: cycloheximide; DDR: DNA damage response; DMEM: Dulbecco's modified Eagle's medium; ERMS: embryonal RMS; FBS: fetal bovine serum; K_{elim} : elimination rate constant; P3F: PAX3-FOXO1; PI: propidium iodide; RMS: rhabdomyosarcoma; RRM: retinoid-related molecules; RT-qPCR: real-time quantitative PCR; TUNEL: terminal deoxy-transferase (TdT)-mediated deoxyuridine triphosphate (dUTP) nick-end labeling

Grant sponsors: Lebanese National Council for Scientific Research (CNRS), American Lebanese Syrian Associated Charities (ALSAC), International Outreach Program at St Jude Children's Research Hospital, Memphis, TN, Children's Cancer Center of Lebanon

DOI: 10.1002/ijc.29886

History: Received 31 July 2015; Accepted 30 Sep 2015; Online 9 Oct 2015

***Correspondence to:** Raya Saab, Pediatric Hematology/Oncology, American University of Beirut, Riad El Solh Street, Beirut 1107 2020, Lebanon, Tel.: +961-1-350000, ext. 4780, Fax: +961-1-377384, E-mail: rs88@aub.edu.lb

approximately 40% of soft tissue sarcomas.^{2,3} RMS likely arises from primitive mesenchymal progenitors that have undergone a limited program of myogenic differentiation, because of the expression of skeletal myogenic proteins in RMS tumors.^{1,4} Rhabdomyosarcoma occurs in two major histological subtypes: embryonal (ERMS) and alveolar (ARMS) histologies.^{1,4} ARMS is associated with a chromosomal translocation between the PAX3 or PAX7 and FOXO1 genes in approximately 55 and 22% of cases, respectively.⁵ Patients presenting with ARMS tumors usually have a worse prognosis as compared to ERMS. The PAX-FOXO1 fusion transcript has been shown to exhibit a more potent transcriptional activation function than the PAX proteins alone,⁶ and contributes to the invasive phenotype of ARMS,^{7,8} making it an interesting target for therapeutic intervention.⁹ Despite multiple attempts at intensifying chemotherapeutic approaches to treatment, limited improvements in survival have been made for patients with advanced-stage disease or recurrent RMS over the past 10 years.¹⁰⁻¹² This underlies the need for novel therapeutic approaches.^{10,13}

Retinoic acid is a morphogen and a major regulator of cellular proliferation, apoptosis and differentiation,¹⁴ and has been investigated as differentiation therapy in multiple types of cancer, contributing to improved outcomes in other primitive tumors of childhood, such as acute promyelocytic leukemia and neuroblastoma.^{15,16} In RMS, retinoic acid has shown

What's new?

Rhabdomyosarcoma (RMS) is an aggressive childhood tumor, and new agents are urgently needed to improve outcome, especially in advanced disease. This study shows that ST1926, a synthetic retinoid, is effective against RMS *in vitro* and *in vivo* at therapeutically relevant concentrations. ST1926 treatment resulted in reduced RMS cell viability and significantly delayed tumor growth in mice, actions that stemmed from ST1926 induction of the DNA damage response and S-phase arrest. The effects were independent of *TP53* mutation status. ST1926 further decreased levels of the PAX-FOXO1 fusion oncoprotein, a possible player in fusion gene-positive RMS tumor cell invasion.

some activity in inhibiting proliferation and inducing differentiation *in vitro*, however the effects are of low magnitude, and do not translate into tumor control *in vivo* in mouse xenograft studies, partly due to incomplete cell cycle exit despite evidence of enhanced differentiation.^{17–20} More potent synthetic retinoids have been developed, and some were found to exhibit mechanisms of action independent of retinoic acid receptor signaling pathway, resulting in growth inhibitory and proapoptotic activity.²¹ Prototypes of atypical retinoids—also known as retinoid-related molecules (RRM)—are CD437 and its analog ST1926,²² which shows more favorable pharmacokinetic profile than CD437 and is orally bioavailable.²³ Both compounds are potent inducers of apoptosis, with antitumor effects in several cancer subtypes^{24,25} and induce massive apoptosis even in ATRA-resistant tumors.²⁶ ST1926 is attracting growing attention because of its unique mechanism of antitumor action, where it has been shown to induce early DNA damage, cell cycle arrest and apoptosis in leukemia and solid tumor cell lines.^{22,24,26–28} In view of the moderate effect of retinoic acid on inhibition of proliferation in RMS cell lines, we decided to investigate the potential efficacy of the more potent retinoid ST1926 in this aggressive tumor, using both ERMS and ARMS cell lines and xenografts in immunodeficient mice.

Material and Methods**Cell lines, growth and treatment conditions**

Human RMS cell lines JR1, Rh30, Rh36 and Rh41 were generously donated by Dr. Peter Houghton (Columbus, OH), and have been previously described (reviewed in Ref. 29). The RD cell line was purchased from ATCC (Manassas, VA). JR1, RD and Rh30 cells were cultured in Dulbecco's modified Eagle's medium (DMEM, Sigma, St. Louis, NO); Rh36 and Rh41 were cultured in RPMI-1640 medium, both supplemented with 10% fetal bovine serum (FBS), 1% L-glutamine and 1% penicillin/streptomycin (all from Sigma). All cells were maintained under standard incubator conditions (humidified atmosphere, 21% O₂, 5% CO₂, 37°C). ST1926 (Biogem, Ariano Irpino, Italy) was dissolved in DMSO, stored protected from light at –80°C and diluted to the final concentrations as needed.

Plasmids and viral transduction

The expression plasmids pMSCV-IRES-GFP and pMSCV-GFP-IRES-PAX3-FOXO1 were kindly donated by Dr. Gerard Grosveld (Memphis, TN). HEK 293T cells (ATCC) were used

for retrovirus production using calcium phosphate transfection with the appropriate respective packaging plasmids. For viral transductions, cells were plated in six-well plates at a density of 200,000 cells per well. Viral supernatant was added to the cells with 8 µg/ml polybrene (hexadimethrine bromide, Sigma). Spinoculation was performed at 32°C, 2,500 rpm for 2 hr and medium was replaced after 3 hr. The following day, the procedure was repeated. GFP-positive cells were sorted using BD FACSAria™ III cell sorter.

Cell viability, cell cycle assays and apoptosis assay

MTT cell viability assay was performed using MTT assay kit (Roche Diagnostics, Indianapolis, IN) according to the manufacturer's instructions. For cell cycle analysis, triplicate plates of each cell line were treated with 1 µM ST1926 or equivalent volume of vehicle. Cells were harvested at the specified time points, fixed in 80% ethanol, incubated with RNase A, then stained with propidium iodide (PI) stain and analyzed for DNA content using FACScan flow cytometer (Becton Dickinson, San Jose, CA). For analysis of bromodeoxyuridine (BrdU) incorporation, cells were treated with ST1926 or vehicle as specified, and then 30 µM BrdU for 2 hr before harvesting. After overnight fixation, cells were treated with 2 N HCL, neutralized by borate buffer and incubated with anti-BrdU primary antibody (Santa Cruz Biotechnology, Santa Cruz, CA) followed by CyTM3-conjugated secondary antibody (Jackson ImmunoResearch Laboratories, West Grove, PA) and analyzed using the FACScan flow cytometer. For terminal deoxy-transferase (TdT)-mediated deoxyuridine triphosphate (dUTP) nick-end labeling (TUNEL) assay, cells were treated with ST1926 or vehicle as specified, and then TUNEL assay (Roche Diagnostics) was performed as per manufacturer's instructions. Studies were performed at least twice, each time using triplicate samples.

Protein expression analysis

Cells were lysed on ice for 15 min in Universal Lysis Buffer as in our previous studies,¹⁷ and protein was quantified by Bradford assay (Bio-Rad, Richmond, CA). Equivalent amounts of protein were fractionated by 6–12% SDS-PAGE and transferred to polyvinylidene difluoride membranes (Bio-Rad). Membranes were probed with antibodies against phosphorylated CHK2, phosphorylated H2AX, phosphorylated ATM, phosphorylated p53, FOXO1 (all from Cell Signaling Technology,

Beverly, MA), p21, GAPDH, CDK1 (all from Santa Cruz Biotechnology) and TUBULIN (Abcam, Cambridge, UK) and then detected with species-specific horseradish peroxidase-coupled secondary antibodies (Santa Cruz Technology) and visualized by enhanced chemiluminescence (Roche) upon detection on X-ray films or Chemidoc machine (Bio-Rad).

Real-time quantitative PCR

RNA was extracted using TRIzol reagent (Ambion, Austin, TX) according to the manufacturer's instructions, followed by treatment with DNase I (Qiagen, Valencia, CA). cDNA synthesis was performed using RevertAid first-strand cDNA synthesis kit (Fermentas, Vilnius, Lithuania). Real-time quantitative PCR (RT-qPCR) was performed using the iQSYBR Green Supermix kit using a CFX96 system (Bio-Rad). Amplification was done using the following primers: GAPDH: Forward 5'-TGGTGCTCAGTGTAGCCCAG-3', Reverse 5'-GGACCTGACCTGCCGTC TAG-3'; PAX3-FOXO1: Forward 5'-GAACCCACCATTGG CAAT-3', Reverse 5'-TCTGCACACGAATGAACTTGCT-3'. RT-qPCR conditions were as follows: 95°C for 15 min for denaturation, 95°C for 15 sec, 72°C for 1 min and annealing at 55°C for 40 cycles.

Cycloheximide chase assay

Cycloheximide (CHX, Sigma) pulse-chase experiment was performed as described in the literature.^{30,31} Cells were seeded in 10-cm plates. After culturing overnight, the cells were treated with vehicle or 1 μ M ST1926 combined with 35 μ M cycloheximide alone or with 35 μ M cycloheximide and 10 nM bortezomib (BZ, LC Laboratories, Woburn, MA). Total protein lysates were collected at planned time points and subjected to immunoblotting as above.

Mouse studies

All mouse studies were approved by the Institutional Care and Use Committee (IACUC) at the American University of Beirut, and all studies followed the IACUC-approved guidelines. Xenografts of Rh41 tumors were generously donated by Dr. Peter Houghton, and were serially passaged *in vivo*. Xenografts for the RD and JR1 cell lines were formed by subcutaneous injections of 1×10^7 cells per injection into the right flank of immunodeficient NOD/SCID mice (NOD.CB17-Prkdc^{scid}/J, Charles River, France), as in our previous studies.¹⁷ Once tumors grew to a volume of at least 150 mm³, treatment was initiated with 20 mg/kg/day of ST1926 or vehicle DMSO control, both diluted in 1:1 cremophor/ethanol solution, by oral gavage for 5 days per week for 2 weeks. Tumor size was monitored by twice weekly measurements with a vernier caliper. Tumor volume was calculated as $[\text{length} \times (\text{width})^2]/2$. Mice were euthanized at the specified time points for tumor harvesting. Tumors were dissected, fixed in 4% paraformaldehyde and embedded in paraffin. Four-micron sections were used for immunohistochemical staining using antiphosphorylated H2AX and antiphosphorylated Ser/Thr (Cell Signaling Technology). Antigen retrieval was performed in a steamer using citrate anti-

gen retrieval buffer (pH 6.0). ABC Elite Kit (Vector Labs, Burlingame, CA) was used for detection by biotinylated secondary antibody and streptavidin conjugated to horseradish peroxidase followed by DAB substrate (DAKO, Glostrup, Denmark).

Pharmacokinetic studies

Pharmacokinetics studies were carried out using mice CD1-Foxn1tm (Charles River). Male CD-1 mice (20–22 g) were used for all studies. Mice received a single dose of ST1926 at 15 mg/kg in 10% of ethanol/cremophor EL (1:1) in saline *via* oral route with a dosing volume of 10 ml/kg. At 0.5, 1, 4 and 8 hr after dose ($n = 3/\text{time point}$), blood was collected into sodium-heparinized test tubes, centrifuged (5 min, 6,000g at 4°C) and the resultant plasma stored at -20°C until analysis. At the time of analysis, plasma samples were thawed and a 50 μ l aliquot was transferred to a 1.5-ml plastic vial and 150 μ l of acetonitrile containing internal standard (IS, 0.25 μ g/ml) was added. The samples were vortex mixed for 1 min, stored at -20°C for 20 min, sonicated for 1 min, vortex mixed for 20 sec and centrifuged at 12,000g for 5 min at 4°C. The resultant supernatant was transferred into autosampler vials and a 10 μ l aliquot was analyzed. Calibration curve (0.05–2.0 μ g/ml) and quality control samples (0.1 and 1.0 μ g/ml) were prepared in blank plasma and analyzed in a similar manner as the unknown samples. The concentration of ST1926 and IS in plasma was determined by liquid chromatography with fluorimetric detection (model UltiMate FLD-3000, ThermoScientific, Rochester, NY). The excitation and emission wavelengths were 330 and 470 nm, respectively. The LC separation used an isocratic mode and a Betasil phenyl column (150 mm \times 4.6 mm; particle size 3 μ m; ThermoScientific) equipped with a ODS guard column (4.0 mm \times 3.0 mm; Phenomenex, Torrance, CA) at room temperature. Mobile phase consisted of 0.1% of aqueous formic acid and acetonitrile (30/70, v/v) with a flow rate of 0.5 ml/min from 0 to 10 min and 1 ml/min from 11 to 20 min. Calibration curves and quality control samples were analyzed concurrently with each set of unknown samples. The calibration curves were linear over the concentration range considered with a correlation coefficient >0.99 in plasma. The limit of quantification measured with acceptable accuracy and precision ($\leq 20\%$) was 0.05 μ g/ml. Accuracy of quality control samples was lower than -10.5% . Standard methods³² were used to calculate the pharmacokinetic parameters using model-independent method. The maximum concentration (C_{max}) and the time to reach C_{max} (T_{max}) were taken from experimental curves. The terminal phase half-life was determined from the elimination rate constant (K_{elim}), calculated by linear regression analysis of the last final points. The area under the curve (AUC) plasma concentration–time profile was calculated by linear trapezoidal rule and extrapolated to infinity using the terminal slope and the last plasma concentration. The apparent clearance in plasma (CL/F) was calculated by dividing the dose by the AUC, and the apparent volume of distribution (V_d/F) was calculated by dividing the apparent clearance by K_{elim} . F corresponds to bioavailability factor.

Imaging and statistical analysis

Digital photomicrographs were obtained using a Zeiss 510 NLO multiphoton/confocal laser scanning microscope. Composite images were constructed using Photoshop CS6 software (Adobe Systems). Comparisons between experimental and control groups were performed using Student's *t*-test, and a *p* value below 0.05 was considered statistically significant.

Results

ST1926 inhibits RMS cell proliferation at concentrations as low as 0.5 μ M

To evaluate the effect of ST1926 on RMS cells, we used three well-described ERMS cell lines (JR1, RD and Rh36) and two well-described ARMS cell lines (Rh30 and Rh41). Using MTT cell viability assay, we found that ST1926 treatment reduced viability of all RMS cell lines in a time-dependent fashion, which was most pronounced after 6 days of treatment; effective doses were as low as 0.5–1 μ M (Fig. 1a). We noted a threshold level of 0.5 μ M with similar growth suppressive effects as tenfold higher concentrations. Microscopic observations of the treated cells also showed a decrease in cell number in all tested cell lines with a variable effect on cell morphology (not shown).

ST1926 concentrations of 1 μ M are achievable *in vivo*

Pharmacokinetic studies were performed to evaluate the achievable *in vivo* concentrations of the drug in mice. First, chromatographic analysis showed that the retention times were approximately 8.6 and 13.2 min for ST1926 and the internal standard, respectively (Fig. 1b). Under fluorimetric acquisition mode, blank plasma yielded relative clean chromatograms without co-eluting interference peaks at the retention time of ST1926 and IS. Typical chromatograms of the blank, spiked and treated plasma are shown in Figure 1b. After a single oral administration of 15 mg/kg ST1926 to male CD-1 mice, we found that the compound was rapidly absorbed in plasma, resulting in a mean maximum concentration (C_{max}) of 3.5 ± 1.01 μ g/ml at 0.5 hr (the first time point collected; T_{max}), corresponding to a 9.43 μ M concentration (Figs. 1c and 1d). Thereafter concentration declined with an apparent half-life of about 1.7 hr (Fig. 1d), and remained above 1 μ M for several hours (Fig. 1c).

In view of these results, taking into consideration the similarity of efficacy profile for concentrations above 0.5 μ M on the tested cell line (see Fig. 1a), and as C_{max} of above 1 μ M was maintained *in vivo* for several hours, we decided to use a 1 μ M ST1926 concentration for all subsequent *in vitro* studies.

ST1926 induces an S-phase arrest in RMS cells at 48 hr

To determine whether the reduction in cell viability induced by ST1926 was associated with cell cycle perturbation, we performed cell cycle analysis by PI staining for DNA content. We found that treatment with ST1926 resulted in accumulation of cells in the G1-phase at 24 hr of treatment in all tested cell

lines, with a corresponding decrease in cells in the G2/M and/or S-phases of the cell cycle (Fig. 2a). Interestingly, by 48 hr, an S-phase arrest was detected in four of the five tested cell lines, the exception being Rh30, where a persistent G1 arrest was observed (Fig. 2b). The observed accumulation of cells in S-phase at 48 hr of treatment was also confirmed by BrdU incorporation assay (Fig. 2c). The cell cycle analysis also showed an increase in proportion of cells with sub-G1 DNA content after ST1926 treatment for 48 hr in some of the cell lines. We therefore explored the possibility that ST1926 was also inducing apoptosis, as previously reported as a mechanism of action for ST1926 in other tumor cell types.^{23,24,28} By TUNEL assay, we found that ST1926 indeed induced apoptosis at 48 hr of treatment in three of four tested cell lines (Fig. 2d). We conclude that ST1926 treatment caused an early accumulation of RMS cells in the G1-phase of the cell cycle at 24 hr of treatment, but by 48 hr resulted in a combination of mild cell accumulation in S-phase and an increase in apoptotic cell death, in most of the tested cell lines.

ST1926 exerts its effect through activation of the DNA damage response pathway, independent of TP53 status

As ST1926 has been shown to induce a DNA damage response (DDR) in other settings,^{26,33,34} we next evaluated whether its effect on RMS cells was mediated through induction of DNA damage. By Western blotting, we found that markers of a DDR were indeed activated as early as 24 hr post-treatment, with phosphorylation of CHK2, H2AX and ATM (Fig. 3a). As p53 is also activated in response to DNA damage, we also assessed the effect of ST1926 on p53 phosphorylation and upregulation of its downstream target CDKN1A (also known as p21^{Cip1}). Although four of the five tested RMS cell lines are known to have either mutation or deletion in *p53*,²⁹ we found that ST1926 did indeed induce p53 phosphorylation in Rh36 (where *p53* is wild-type) and in JR1, Rh30 and RD cell lines (where *p53* is mutated), while it was absent in the remaining cell line (Rh41) (Fig. 3a). The downstream effector of p53 in cell cycle arrest, p21^{Cip1}, was upregulated at 24 hr in response to ST1926 in Rh30, RD and Rh36 cell lines, while it remained undetected in the remaining cell lines (Rh41 and JR1) (Fig. 3a). The effects on p53 phosphorylation and p21 induction remained similar after 48 hr of treatment (Fig. 3b). Thus, we conclude that ST1926 induces a DDR in all RMS cell lines tested, and the p53 pathway is engaged in cell lines that have intact or expressed p53 protein.

We next evaluated whether activation of the DDR pathway was in fact necessary for the cell cycle arrest induced by ST1926. Co-treatment of RMS cells with ST1926 and caffeine, which is known to inhibit the ATM and ATR kinases necessary for activation of the DDR pathway,³⁵ attenuated the DDR activation induced by ST1926 treatment, shown by decreased phosphorylation of H2AX, CHK2 and p53 (Fig. 3c). Indeed, we found that treatment with caffeine also attenuated the S-phase arrest induced by ST1926 (Fig. 3d), confirming that the cell cycle arrest depends on induction of the DDR.

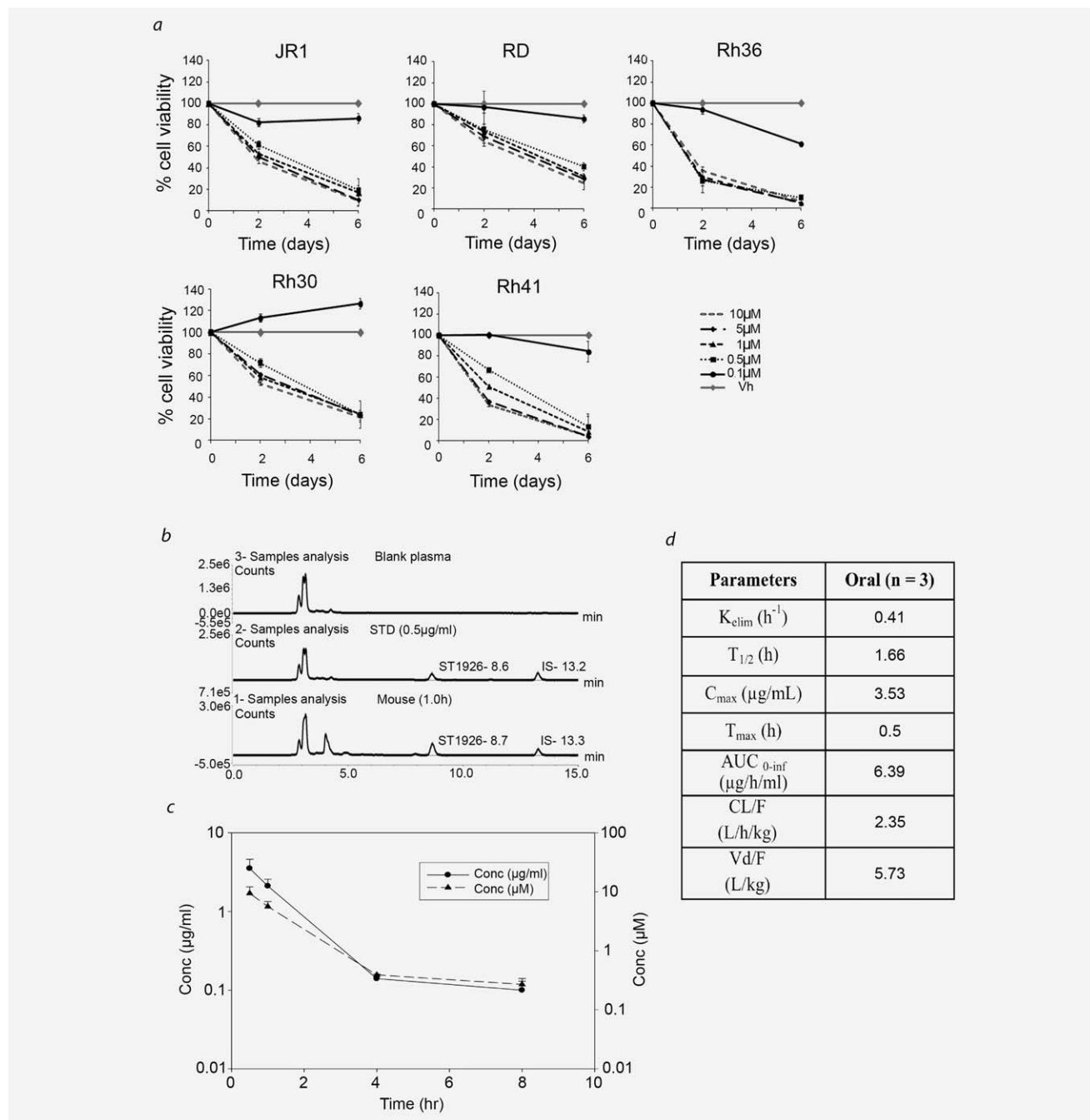


Figure 1. ST1926 decreases cell viability of RMS cell lines. (a) Effects of ST1926 on the viability of ERMS (JR1, RD and Rh36) and ARMS (Rh30 and Rh41) cell lines were assessed using MTT assay. All RMS cells were seeded in 96-well plates and treated with 0.01% DMSO or the indicated concentrations of ST1926 (0.1, 0.5, 1, 5 and 10 μM) for 6 days. Each point represents the mean relative to the control vehicle-treated condition (0.1% DMSO); bars represent standard deviation (n of at least 2, each done in triplicate). Asterisks denote a statistically significant difference (p values < 0.05). (b) Representative HPLC chromatogram of blank plasma (top), plasma spiked with 0.5 $\mu g/ml$ of ST1926 (middle) and plasma from a mouse at 0.5 hr after oral administration of ST1926 (15 mg/kg) (bottom). (c) Plasma concentration–time profile of ST1926 in mice after its oral administration (15 mg/kg); each point and bar represent the mean \pm standard deviation ($n = 3$). The values are expressed in $\mu g/ml$ (circle) or μM (triangle). (d) Pharmacokinetic parameters of ST1926 following a single oral dose of 15 mg/kg in CD1 mice.

Interestingly, ST1926 treatment also resulted in a decrease in protein levels of CDK1 (Fig. 4a), which is known to occur downstream of DDR activation and may contribute to the execution of the S-phase arrest.³⁶

ST1926 decreases protein levels of the fusion oncoprotein PAX3-FOXO1 in ARMS cells

As the fusion oncoprotein PAX3-FOXO1 (P3F) has been shown to contribute to the survival and invasive properties of

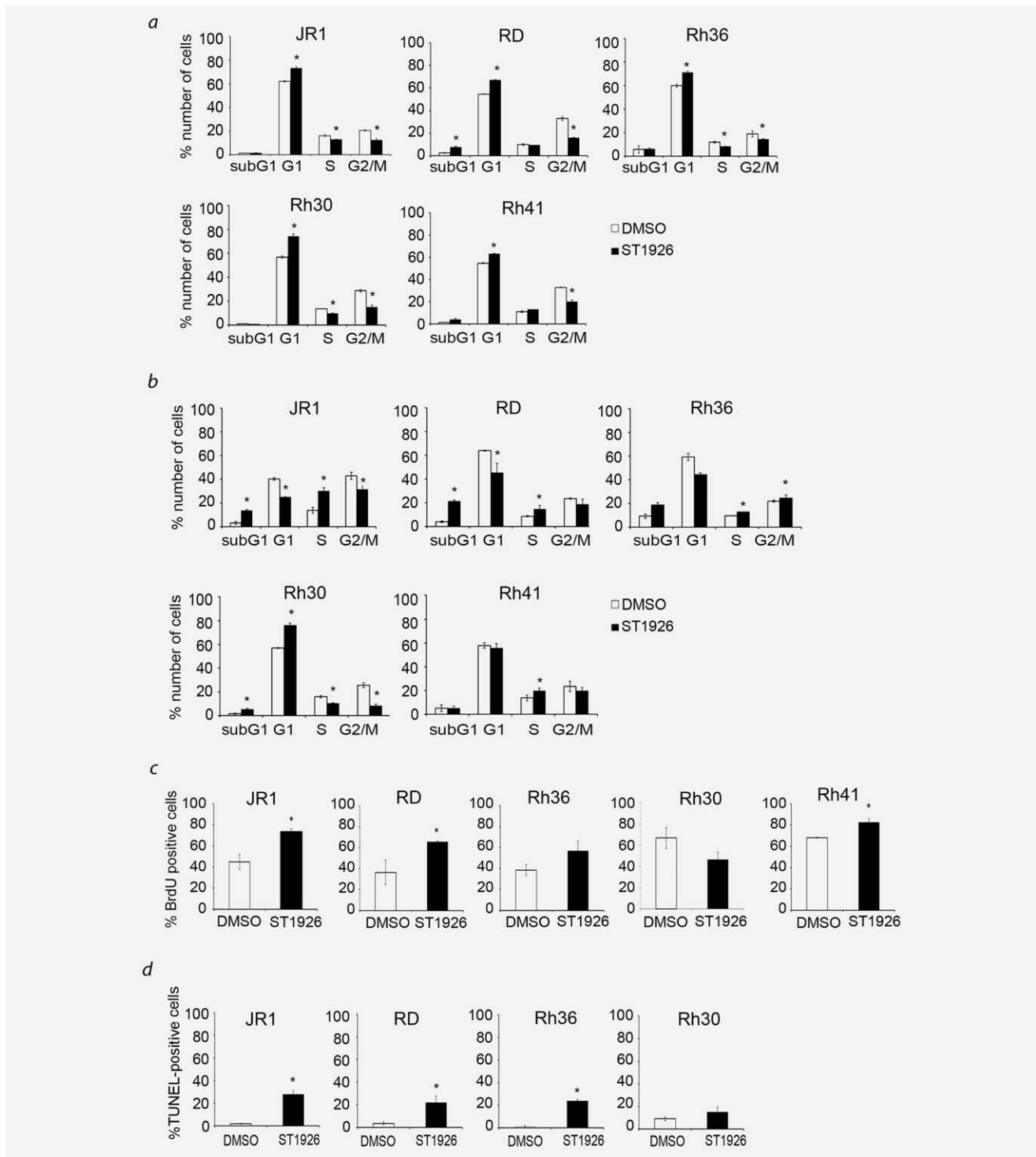


Figure 2. ST1926 induces cell cycle arrest in RMS cells. Cell cycle analysis of RMS cells treated with vehicle (0.01% DMSO) or 1 μ M ST1926, as indicated, for (a) 24 hr and (b) 48 hr. Graphs are representative of three independent experiments, each done in triplicate. Bars represent standard deviation. Asterisks denote a statistically significant difference (p values < 0.05). (c) BrdU incorporation assay in the indicated RMS cells treated with vehicle (0.01% DMSO) or 1 μ M ST1926, as indicated, for 48 hr. Graphs are representative of at least two independent experiments, each done in triplicate; bars represent standard deviation. Asterisks denote a statistically significant difference (p values < 0.05). Rh36 has a p value = 0.07. (d) TUNEL assay in the indicated RMS cells after 48 hr of treatment with vehicle (0.01% DMSO, white bars) or 1 μ M ST1926 (black bars). Graphs are representative of at least two independent experiments, each done in triplicate. Bars represent standard deviation. Asterisks indicate p values < 0.05.

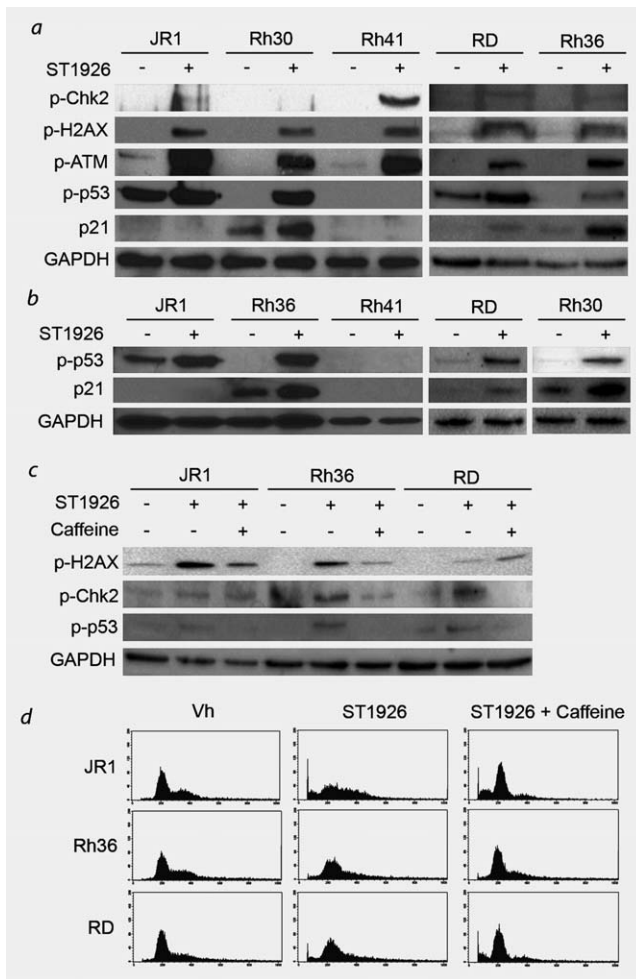


Figure 3. ST1926 acts through induction of a DNA damage response in RMS cells. Western blot analysis of the indicated proteins in the indicated RMS cell lines after (a) 24 hr and (b) 48 hr of treatment with ST1926 or vehicle, as shown. (c) Western blot analysis of expression of the indicated DDR proteins at 24 hr of treatment in RMS cells treated with vehicle, 1 μM ST1926 or 1 μM ST1926 and 4 μM caffeine, as indicated. (d) Cell cycle analysis by PI/FACS of the indicated RMS cells treated with vehicle, 1 μM ST1926 or 1 μM ST1926 and 4 μM caffeine, as indicated.

ARMS cells, we investigated whether ST1926 treatment affected the expression of P3F. Interestingly, we found that protein levels of P3F were decreased after 48 hr of treatment with ST1926 (Figs. 4a and 4b). This was not due to transcriptional regulation, as RT-qPCR showed no decrease in *PAX3-FOXO1* transcript levels in treated cells (Fig. 4c). In addition, we transduced embryonal JR1 RMS cells with a lentiviral vector constitutively expressing P3F, and found that treatment of P3F-expressing JR1 cells with ST1926 also decreased the protein levels of P3F (Fig. 4d), further supporting control at a post-transcriptional level.

To evaluate whether ST1926 might be enhancing proteosomal degradation of P3F, we performed a cycloheximide (CHX) chase assay,³⁰ with or without proteosomal inhibition using bortezomib (BZ).³¹ Pulse-chase assays using CHX are

useful to monitor the effects of drugs on protein degradation, where CHX is used to inhibit protein synthesis, and protein levels are then monitored to evaluate rates of degradation.³⁰ We combined CHX with BZ (to inhibit proteosomal protein degradation) and then evaluated whether the observed decrease in protein levels occurs *via* the proteosomal pathway.³¹ Using this approach in Rh30 cells, we found that the ST1926-induced decrease in P3F levels by 24 hr of treatment occurred earlier upon CHX treatment of cells (Fig. 4e, compare upper control and middle CHX-treated panels, lanes e–g to lanes b–d, respectively), as expected due to inhibition of protein synthesis. Further treatment with BZ reversed this effect, and normalized levels of P3F in ST1926-treated cells such that they resembled levels in vehicle-treated controls (Fig. 4e, lower CHX + BZ-treated panels, compare lanes f and g to lanes c and d, respectively). From these studies, we conclude that ST1926 decreases levels of P3F in ARMS cells at a post-transcriptional level by enhancing proteosomal degradation of the protein.

ST1926 retards RMS xenograft growth *in vivo*

To evaluate the efficacy of ST1926 *in vivo*, we treated cohorts of mice carrying xenografts of the ERMS cell lines JR1 and RD, and the ARMS cell line Rh41. Once xenografts reached a size of >150 mm³, mice were treated orally with ST1926 (20 mg/kg) or vehicle, for five consecutive days per week for 2 weeks. ST1926 treatment at this dose was well tolerated by mice, as also shown by previous studies,^{23,24} although we observed mild weight loss in treated animals (data not shown). Significant delay in tumor growth was observed in RD and Rh41 xenografts as early as 4 and 8 days of treatment, respectively, and by Day 11 in JR1 tumors (Fig. 5a). Similar to the findings *in vitro*, evaluation of the tumor xenografts showed that tumors from ST1926-treated mice had an induction of a DDR, as evidenced by enhanced protein levels of phosphorylated H2AX, and increased phosphorylation of ATM and ATR target proteins, detected by immunostaining for phosphorylated serine/threonine residues (pS/T) (Fig. 5b).

Discussion

In view of the tolerability of ST1926 and its oral bioavailability, this synthetic retinoid presents a promising novel therapeutic agent. In a panel of RMS cell lines, we have now shown that ST1926 is efficacious in inducing growth inhibition at pharmacologically achievable concentrations. In addition, treatment of RMS xenografts in immunodeficient mice was tolerable, and resulted in clinical benefit with decrease in rate of tumor growth.

While retinoids have been used as differentiation therapy in acute promyelocytic leukemia and in neuroblastoma,^{15,16} and have been investigated in other tumors including RMS,^{17–20} this is the first study to evaluate the use of the novel retinoid ST1926 in RMS. We found that ST1926 effectively inhibits both ERMS and ARMS cell proliferation, exerting its effects by activating the DDR pathway, resulting in a

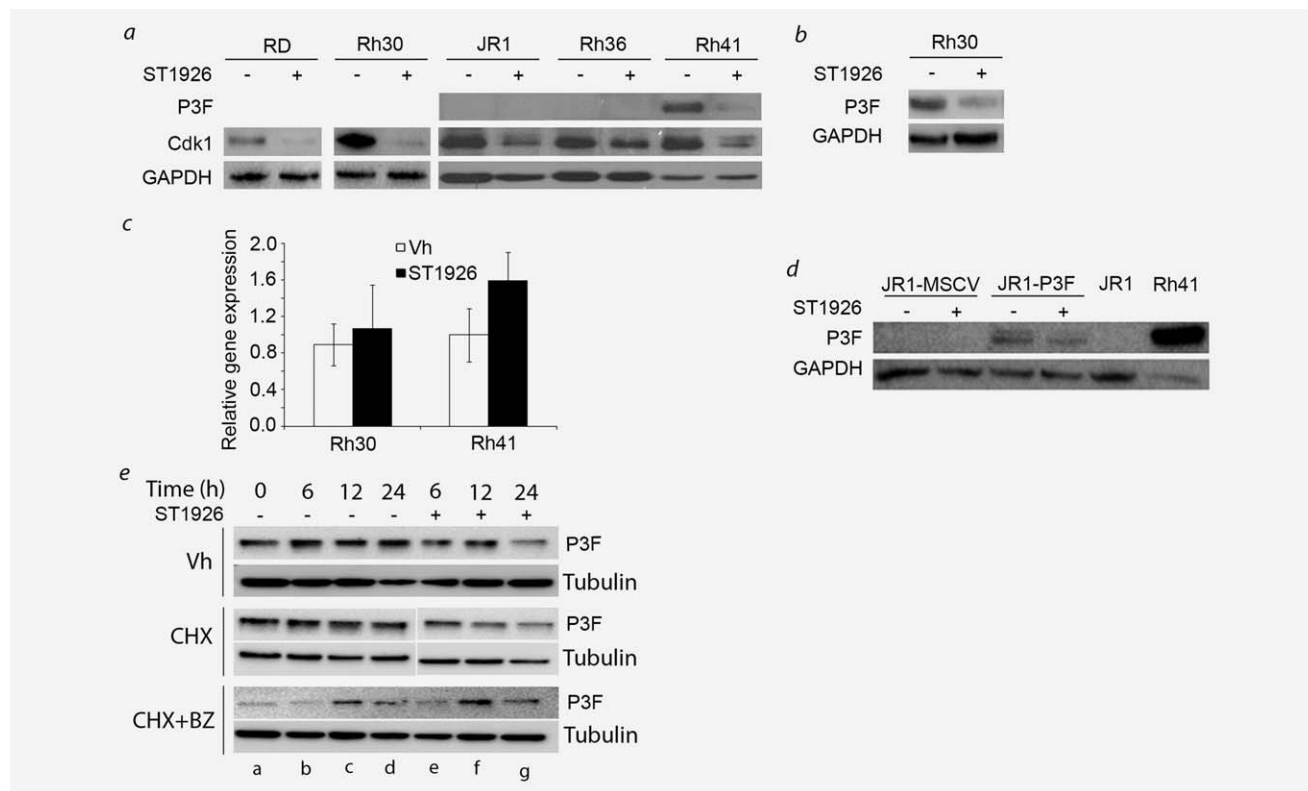


Figure 4. ST1926 decreases protein levels of CDK1 and PAX3-FOXO1 (P3F) in RMS cells. (a) and (b) Western blot analyses of the indicated proteins in the specified RMS cell lines after 48 hr of treatment with ST1926 or vehicle, as shown. GAPDH was used as a loading control. (c) RT-qPCR analysis of *P3F* mRNA levels after 48 hr of treatment of the indicated ARMS cells with either vehicle (Vh, white bars) or ST1926 (black bars), as shown. Gene expression is shown as relative to expression of the housekeeping gene *GAPDH*. Graphs are representative of at least two independent experiments, each done in triplicate. Bars represent standard deviation. Asterisks indicate p values < 0.05 . (d) Western blotting for the indicated proteins in lysates of JR1 cells transduced either with empty vector (JR1-MSCV) or PAX3-FOXO1-expressing vector (JR1-P3F), and treated with vehicle or ST1926, as indicated. Nontransduced JR1 cell lysate (JR1) was used as a negative control, and Rh41 (ARMS) cell lysate as a positive control. GAPDH was used as a loading control. (e) Western blotting for the indicated proteins in lysates of Rh30 cells after pulse-chase assay using cycloheximide and bortezomib, as indicated. Cells were treated with vehicle or ST1926 for the indicated hours. Tubulin was used as a loading control.

combination of S-phase arrest and inhibition of cell cycle progression, and induction of apoptosis. This is similar to its mechanism of action in other cancer cell lines, including leukemia^{24,28,33,37} and some solid tumors.^{21,26,27} In our study, ST1926 induced a prominent DDR both in treated RMS cells *in vitro* and in xenografts *in vivo*, with phosphorylation of H2AX, ATM and ATR substrates, as well as p53 protein. The effects of ST1926 were dependent on DDR activation, as caffeine treatment abolished both the DDR and S-phase arrest. The DDR-induced S-phase arrest was accompanied by a concomitant decrease in levels of CDK1, an essential kinase for progression through the G2/M phase of the cell cycle.³⁶ This decrease in CDK1 is in agreement with previously reported transcriptional control of CDK1 by components of the DDR pathway.³⁸

Importantly, we found that the efficacy of ST1926 was independent of the status of *p53* in the tested RMS cell lines. *p53* is a central regulator of both cell cycle arrest and apoptosis in response to DNA damage, and *p53* mutations or path-

way aberrations are common in most cancers.^{39,40} In RMS, *p53* mutations are less common; however, they occur at a higher frequency in relapsed and/or resistant tumors.⁴ Thus, the efficacy of ST1926 irrespective of *p53* mutational status is very appealing for treatment of relapsed and resistant tumors where the *p53* pathway may be compromised. Also of interest, we found that ST1926 decreased the protein levels of the oncogenic fusion protein PAX3-FOXO1 in both tested ARMS cell lines by post-translational modulation. This finding is especially promising as the fusion protein has been implicated in many of the invasive properties of ARMS cells.^{6,41} Our findings showed that the effects of ST1926 on reduction of PAX3-FOXO1 protein levels occurred through enhancing its protein degradation *via* the proteasomal pathway. The proteasome was recently suggested to be implicated in the mode of action of ST1926 in acute myeloid leukemia cells,³³ while ST1926-induced cell death in chronic myeloid leukemia and reduced BCR-ABL oncoprotein levels were shown to be independent of the proteasome.²⁸ Whether the effect of

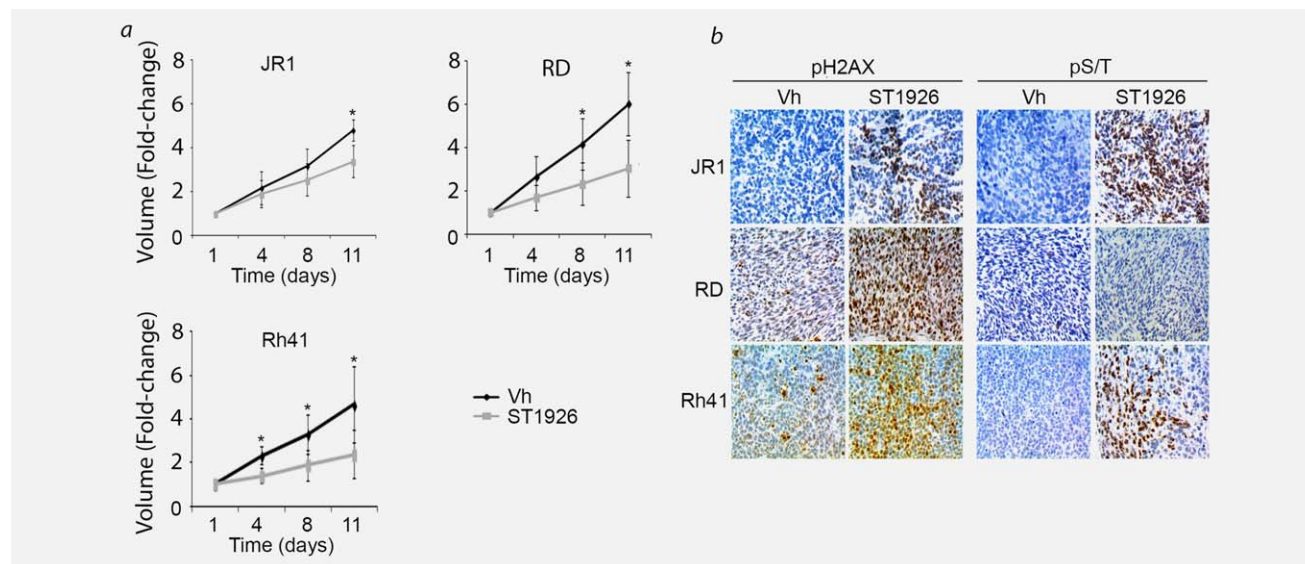


Figure 5. ST1926 inhibits RMS xenograft tumor growth *in vivo*. (a) Volume of the indicated RMS tumors in xenograft-carrying mice after oral treatment with either vehicle (Vh, black) or ST1926 (gray), at the indicated days after treatment initiation. Volumes are expressed as a percentage of tumor volume measured at Day 1. Bars represent standard deviation. Four to seven mice were used in each cohort. Asterisks indicate p values < 0.05 . (b) Immunohistochemical staining for the indicated proteins in RMS tumor xenografts treated with either vehicle (Vh) or ST1926, as indicated.

ST1926 on the proteasome pathway precedes or is consequent to the apoptotic response remains to be elucidated, as the proteasome pathway has been shown to be activated downstream of the apoptotic response.^{42,43}

As ST1926 has already shown clear-cut antitumor activity in several animal tumor models,^{24,28,37} we asked whether the compound achieved an adequate plasma concentration in mice. When a single dose of ST1926 (15 mg/kg) was orally administered to male CD-1 mice, the compound appeared rapidly in plasma and was present until 8 hr after dosing. We found that the apparent plasma clearance of ST1926 was 2.35 l/h/kg, which represents 80% of liver plasma flow in mice,⁴⁴ suggesting a main role of the liver on disposition of the compound. Interestingly, we found a high apparent volume of distribution (5.73 l/kg), greater than the expected mouse blood volume of 0.085 l/kg,⁴⁴ indicating significant extravascular distribution of the compound, which likely contributes to the observed *in vivo* antitumor activity of ST1926. In our mouse xenograft studies, ST1926 had an inhibitory effect on tumor growth in both ERMS (RD, JR1) and ARMS (Rh30) tumors. The observed prominent DDR activation in treated RMS xenografts also showed that the drug was able to reach its target and exert its molecular effect locally. The observed retardation of tumor growth after ST1926 treatment *in vivo* is encouraging, and suggests that ST1926 may be a useful agent for investigation in RMS, possibly in combination therapy to try to effect even better tumor control.

Of note, an oral formulation of ST1926 was tested in a Phase I trial for patients with ovarian cancer.⁴⁵ No major toxicities were encountered. However, it was found that the drug underwent major glucuro-conjugation, negatively

influencing its bioavailability. After this trial, efforts in further clinical development of ST1926 focused on formulations to reduce its glucuro-conjugation, which occurs on the phenolic hydroxyl group on ST1926 structure, and acts as a major mechanism of its fast excretion in humans. In that regard, ST1926 analogues that are less amenable to glucuro-conjugation have recently been synthesized,⁴⁶ and at least one of these derivatives, named ST5589, has now shown antitumor activity in lymphoma preclinical models, phenocopying the preclinical activity of ST1926.⁴⁷ In addition, an alternative mechanism to prolong plasma half-life using the parent ST1926 compound is to encapsulate it in nanoparticles protecting it from glucuro-conjugation occurring in the liver, thereby enhancing its tissue biodistribution. Our findings of activity of the parent ST1926 compound and its mechanism of action in preclinical models of RMS identify this drug as of possible interest in clinical trials in patients with RMS, to be tested in a setting where bioavailability is improved by one of the above discussed methods.

In conclusion, our findings indicate that the novel adamantyl retinoid ST1926 is effective in inhibiting RMS cell proliferation *in vitro* and *in vivo* by inducing a DDR-mediated S-phase arrest. Reduction in CDK1 protein levels and a decrease in the PAX3-FOXO1 oncogenic fusion protein in ARMS may both play a role in mediating its effects. We propose that ST1926 should be further developed in clinical trials of RMS, alone or in combination with other agents such as topoisomerase inhibitors, where the effect on S-phase arrest and cell death would be expected to be more pronounced in combination therapy.

Acknowledgements

The authors thank Dr. Antonio Iorio for technical assistance in analytical method development and pharmacokinetic studies, Miss Maria O. Esmerian for helping with the flow cytometry acquisitions, Mr. Raed Hmadi for assis-

tance in preparation of the retinoid formulation and the core facilities at the AUBMC for technical and infrastructure support. They also thank Dr. Peter Houghton for RMS cells lines and Dr. Gerard Grosveld for the pMSCV-IRES-GFP-Pax3-FKHR plasmid.

References

- Saab R, Spunt SL, Skapek SX. Myogenesis and rhabdomyosarcoma the Jekyll and Hyde of skeletal muscle. *Curr Top Dev Biol* 2011;94:197–234.
- Spunt SL, Pappo AS. Childhood nonrhabdomyosarcoma soft tissue sarcomas are not adult-type tumors. *J Clin Oncol* 2006;24:1958–9; author reply 9–60.
- Stuart A, Radhakrishnan J. Rhabdomyosarcoma. *Indian J Pediatr* 2004;71:331–7.
- Merlino G, Helman LJ. Rhabdomyosarcoma—working out the pathways. *Oncogene* 1999;18:5340–8.
- Sorensen PH, Lynch JC, Qualman SJ, et al. PAX3-FKHR and PAX7-FKHR gene fusions are prognostic indicators in alveolar rhabdomyosarcoma: a report from the children's oncology group. *J Clin Oncol* 2002;20:2672–9.
- Bennicelli JL, Edwards RH, Barr FG. Mechanism for transcriptional gain of function resulting from chromosomal translocation in alveolar rhabdomyosarcoma. *Proc Natl Acad Sci USA* 1996;93:5455–9.
- Linardic CM. PAX3-FOXO1 fusion gene in rhabdomyosarcoma. *Cancer Lett* 2008;270:10–18.
- Parham DM, Barr FG. Classification of rhabdomyosarcoma and its molecular basis. *Adv Anat Pathol* 2013;20:387–97.
- Olanich ME, Barr FG. A call to ARMS: targeting the PAX3-FOXO1 gene in alveolar rhabdomyosarcoma. *Expert Opin Ther Targets* 2013;17:607–23.
- Raney B, Huh W, Hawkins D, et al. Outcome of patients with localized orbital sarcoma who relapsed following treatment on Intergroup Rhabdomyosarcoma Study Group (IRSG) Protocols-III and -IV, 1984-1997: a report from the Children's Oncology Group. *Pediatr Blood Cancer* 2013;60:371–6.
- Hawkins DS, Gupta AA, Rudzinski ER. What is new in the biology and treatment of pediatric rhabdomyosarcoma? *Curr Opin Pediatr* 2014;26:50–6.
- Perkins SM, Shinohara ET, DeWees T, et al. Outcome for children with metastatic solid tumors over the last four decades. *PLoS One* 2014;9:e100396.
- Barr FG. New treatments for rhabdomyosarcoma: the importance of target practice. *Clin Cancer Res* 2012;18:595–7.
- Gudas LJ. Emerging roles for retinoids in regeneration and differentiation in normal and disease states. *Biochim Biophys Acta* 2012;1821:213–21.
- Reynolds CP, Matthey KK, Villablanca JG, et al. Retinoid therapy of high-risk neuroblastoma. *Cancer Lett* 2003;197:185–92.
- Masetti R, Biagi C, Zama D, et al. Retinoids in pediatric onco-hematology: the model of acute promyelocytic leukemia and neuroblastoma. *Adv Ther* 2012;29:747–62.
- Al-Tahan A, Sarkis O, Harajly M, et al. Retinoic acid fails to induce cell cycle arrest with myogenic differentiation in rhabdomyosarcoma. *Pediatr Blood Cancer* 2012;58:877–84.
- Barlow JW, Wiley JC, Mous M, et al. Differentiation of rhabdomyosarcoma cell lines using retinoic acid. *Pediatr Blood Cancer* 2006;47:773–84.
- Ricaud S, Vernus B, Bonniou A. Response of human rhabdomyosarcoma cell lines to retinoic acid: relationship with induction of differentiation and retinoic acid sensitivity. *Exp Cell Res* 2005;311:192–204.
- Crouch GD, Helman LJ. All-trans-retinoic acid inhibits the growth of human rhabdomyosarcoma cell lines. *Cancer Res* 1991;51:4882–7.
- Milli A, Perego P, Beretta GL, et al. Proteomic analysis of cellular response to novel proapoptotic agents related to atypical retinoids in human IGROV-1 ovarian carcinoma cells. *J Proteome Res* 2011;10:1191–207.
- Cincinelli R, Dallavalle S, Merlini L, et al. A novel atypical retinoid endowed with proapoptotic and antitumor activity. *J Med Chem* 2003;46:909–12.
- Garattini E, Gianni M, Terao M. Retinoid related molecules an emerging class of apoptotic agents with promising therapeutic potential in oncology: pharmacological activity and mechanisms of action. *Curr Pharm Des* 2004;10:433–48.
- El Hajj H, Khalil B, Ghandour B, et al. Preclinical efficacy of the synthetic retinoid ST1926 for treating adult T-cell leukemia/lymphoma. *Blood* 2014;124:2072–80.
- Valli C, Paroni G, Di Francesco AM, et al. Atypical retinoids ST1926 and CD437 are S-phase-specific agents causing DNA double-strand breaks: significance for the cytotoxic and antiproliferative activity. *Mol Cancer Ther* 2008;7:2941–54.
- Di Francesco AM, Meco D, Torella AR, et al. The novel atypical retinoid ST1926 is active in ATRA resistant neuroblastoma cells acting by a different mechanism. *Biochem Pharmacol* 2007;73:643–55.
- Zuco V, Zanchi C, Cassinelli G, et al. Induction of apoptosis and stress response in ovarian carcinoma cell lines treated with ST1926, an atypical retinoid. *Cell Death Differ* 2004;11:280–9.
- Nasr RR, Hmadi RA, El-Eit RM, et al. ST1926, an orally active synthetic retinoid, induces apoptosis in chronic myeloid leukemia cells and prolongs survival in a murine model. *Int J Cancer* 2015;137:698–709.
- Hinson AR, Jones R, Crose LE, et al. Human rhabdomyosarcoma cell lines for rhabdomyosarcoma research: utility and pitfalls. *Front Oncol* 2013;3:183.
- Liu R, Zheng HQ, Zhou Z, et al. KLF5 promotes breast cell survival partially through fibroblast growth factor-binding protein 1-pERK-mediated dual specificity MKP-1 protein phosphorylation and stabilization. *J Biol Chem* 2009;284:16791–8.
- Rizzatti EG, Mora-Jensen H, Weniger MA, et al. Noxa mediates bortezomib induced apoptosis in both sensitive and intrinsically resistant mantle cell lymphoma cells and this effect is independent of constitutive activity of the AKT and NF-kappaB pathways. *Leuk Lymphoma* 2008;49:798–808.
- Gibaldi M, Perrier D. Pharmacokinetics, 2nd edn. New York: Marcel Dekker, Inc., 1982.
- Fratelli M, Fisher JN, Paroni G, et al. New insights into the molecular mechanisms underlying sensitivity/resistance to the atypical retinoid ST1926 in acute myeloid leukaemia cells: the role of histone H2A.Z, cAMP-dependent protein kinase A and the proteasome. *Eur J Cancer* 2013;49:1491–500.
- Zuco V, Benedetti V, De Cesare M, et al. Sensitization of ovarian carcinoma cells to the atypical retinoid ST1926 by the histone deacetylase inhibitor, RC307: enhanced DNA damage response. *Int J Cancer* 2010;126:1246–55.
- Zhou BB, Chaturvedi P, Spring K, et al. Caffeine abolishes the mammalian G(2)/M DNA damage checkpoint by inhibiting ataxia-telangiectasia-mutated kinase activity. *J Biol Chem* 2000;275:10342–8.
- Hasegawa H, Ishibashi K, Kubota S, et al. Cdk1-mediated phosphorylation of human ATF7 at Thr-51 and Thr-53 promotes cell-cycle progression into M phase. *PLoS One* 2014;9:e116048.
- Garattini E, Parrella E, Diomede L, et al. ST1926, a novel and orally active retinoid-related molecule inducing apoptosis in myeloid leukemia cells: modulation of intracellular calcium homeostasis. *Blood* 2004;103:194–207.
- Nagarajan A, Dogra SK, Liu AY, et al. PEA15 regulates the DNA damage-induced cell cycle checkpoint and oncogene-directed transformation. *Mol Cell Biol* 2014;34:2264–82.
- Leroy B, Anderson M, Soussi T. TP53 mutations in human cancer: database reassessment and prospects for the next decade. *Hum Mutat* 2014;35:672–88.
- Muller PA, Vousden KH. Mutant p53 in cancer: new functions and therapeutic opportunities. *Cancer Cell* 2014;25:304–17.
- Mercado GE, Barr FG. Fusions involving PAX and FOX genes in the molecular pathogenesis of alveolar rhabdomyosarcoma: recent advances. *Curr Mol Med* 2007;7:47–61.
- Grimm LM, Goldberg AL, Poirier GG, et al. Proteasomes play an essential role in thymocyte apoptosis. *EMBO J* 1996;15:3835–44.
- Hirsch T, Dallaporta B, Zamzami N, et al. Proteasome activation occurs at an early, premitochondrial step of thymocyte apoptosis. *J Immunol* 1998;161:35–40.
- Davies B, Morris T. Physiological parameters in laboratory animals and humans. *Pharm Res* 1993;10:1093–5.
- Sala F, Zucchetti M, Bagnati R, et al. Development and validation of a liquid chromatography-tandem mass spectrometry method for the determination of ST1926, a novel oral antitumor agent, adamantyl retinoid derivative, in plasma of patients in a Phase I study. *J Chromatogr B Analyt Technol Biomed Life Sci* 2009;877:3118–26.
- Giannini G, Brunetti T, Battistuzzi G, et al. New retinoid derivatives as back-ups of Adarotene. *Bioorg Med Chem* 2012;20:2405–15.
- Bernasconi E, Gaudio E, Kwee I, et al. The novel atypical retinoid ST5589 down-regulates Aurora Kinase A and has anti-tumour activity in lymphoma pre-clinical models. *Br J Haematol* 2015 doi: 10.1111/bjh.13595. [Epub ahead of print]